EARTHQUAKE ENGINEERING AND STRUCTURAL DYNAMICS
Earthquake Engng Struct. Dyn. 2004; **33**:465–484 (DOI: 10.1002/eqe.359)

Optimal design of added viscoelastic dampers and supporting braces

Ji-Hun Park[1], Jinkoo Kim[2,*,†] and Kyung-Won Min[3]

[1]*MIDASIT Co., Ltd, IT Venture Tower East Wing 11F, Garak-Dong, Songpa-Gu, Seoul, Korea*
[2]*Department of Architectural Engineering, Sungkyunkwan University, Chunchun-Dong, Jangan-Gu, Suwon 440-746, Korea*
[3]*Department of Architectural Engineering, Dankook University, Seoul, Korea*

SUMMARY

This paper presents a simultaneous optimization procedure for both viscoelastic dampers (VEDs) and supporting braces installed in a structure. The effect of supporting braces on the control efficiency of VEDs is also investigated. To apply a general gradient-based optimization algorithm, closed-form expressions for the gradients of objective function and constraints are derived. Also, the constraint on the dynamic behavior of a structure is embedded in the gradient computation procedure to reduce the number of variables in the optimization. From numerical analysis of an example structure, it was found that when sufficient stiffness cannot be provided for the supporting braces, the flexibility of the brace should be taken into account in the design of the VED to achieve the desired performance of the structure. It was also observed that, as a result of the proposed optimization process, the size of the supporting brace could be reduced while the additional VED size (to compensate for the loss of the control effect) was insignificant. Copyright © 2003 John Wiley & Sons, Ltd.

KEY WORDS: viscoelastic dampers; supporting braces; optimization; passive control

INTRODUCTION

The viscoelastic damper (VED) is acknowledged as one of the most efficient energy absorbing devices for building structures against dynamic loads such as earthquake or wind. Previous studies have shown that the efficiency of an added VED can be greatly enhanced by applying properly sized dampers to proper locations. Zhang and Soong [1] and Shukla and Datta [2] have proposed optimal design methods based on the sequential placement of unit dampers to

*Correspondence to: Jinkoo Kim, Department of Architectural Engineering, Sungkyunkwan University, Chunchun-Dong, Jangan-Gu, Suwon 440-746, Korea.
†E-mail: jinkoo@skku.ac.kr

Contract/grant sponsor: National Research Laboratory Program, Ministry of Science and Technology, Korea; contract/grant number: M1-0203-00-0068

Received 10 December 2002
Revised 15 August 2003
Accepted 17 September 2003

determine the optimal location and size of the VED. Gluck *et al*. [3] have obtained story-wise optimum damping distribution using the solution for the linear quadratic regulator problem. In addition, Loh *et al*. [4] have proposed two design methods based on control theory: one is derived from the linear quadratic regulator, and the other from modal control theory. Tsuji and Nakamura [5] have proposed a unified optimization procedure of both structure and dampers. Using the technique, they have minimized total story-stiffness of a structure satisfying constraints on inter-story drifts. Also, Takewaki [6] and Singh and Moreschi [7] have used a gradient-based approach to obtain optimum distribution of damping devices. Recently Singh and Moreschi [8] have used a genetic algorithm to determine the optimal size and location of viscous dampers and VEDs. Hwang *et al*. [9] have proposed a gradient-based optimization procedure for added damping devices to achieve the same fundamental modal damping ratio as that of the actively controlled structure.

In practice, the VED is installed in a structure by being connected to steel braces. In most studies, however, the braces are assumed to have infinite stiffness compared to the dampers, and are neglected in the analysis procedure. Frequently, however, the cross-sectional size of supporting braces needs to be limited for functional or aesthetic reasons. Also, it is common practice to hide the VED inside of thin partition walls. In this case the effect of the flexible brace needs to be investigated. Fu and Kasai [10] have investigated the interaction between added dampers and supporting braces through parametric study, and proposed a proper ratio between the parameters of the damper and the stiffness of the brace. Their study, however, is mainly based on the study of single-degree-of-freedom systems. In addition, in the application to a multi-degree-of-freedom system, the optimum design of added dampers is conducted assuming that the amount of dampers installed in each story is the same. Takewaki and Yoshitomi [11] have also proposed an optimization procedure for viscous dampers taking the stiffness of braces into account. In their study, however, the stiffness of each brace is assumed to be the same and is excluded from the design variables. Furthermore, only the fundamental mode of vibration is considered in the design process.

This study proposes a procedure for determining optimum parameters of VEDs and their supporting braces. Constraints are imposed on every mean maximum story drift as the practical measure of structural responses. Closed-form expressions for the derivatives of the Lagrangian with respect to design variables are derived for the efficient acquisition of the solution. The Kanai–Tagimi filter is used to model the earthquake ground motion. For the modeling of the structure, state equations are formulated separately for both the model structure and the damper–brace system, and then the two equations are combined to form augmented state equations for the overall system. To demonstrate the application of the proposed approach, the results of the numerical analysis for an 8-story shear building with added VED are presented.

STATE SPACE FORMULATION OF A STRUCTURE WITH VED

State space representation of a structure

The dynamic behavior of a structure is modeled by the state space equation in which the covariance of structural responses for white noise excitation can be obtained algebraically.

The state equation and the output equation are given by

$$\begin{Bmatrix} \dot{\mathbf{q}} \\ \ddot{\mathbf{q}} \end{Bmatrix} = \begin{bmatrix} \mathbf{0} & \mathbf{I} \\ \mathbf{M}^{-1}\mathbf{K} & -\mathbf{M}^{-1}\mathbf{D} \end{bmatrix} \begin{Bmatrix} \mathbf{q} \\ \dot{\mathbf{q}} \end{Bmatrix} + \begin{bmatrix} \mathbf{0} \\ -\mathbf{l} \end{bmatrix} \ddot{x}_g \tag{1}$$

$$\mathbf{y} = [\mathbf{T}_y \;\; \mathbf{0}] \begin{Bmatrix} \mathbf{q} \\ \dot{\mathbf{q}} \end{Bmatrix} \tag{2}$$

where $\mathbf{q}$ and $\mathbf{y}$ are the relative displacement and the inter-story drift of each story, respectively, $\ddot{x}_g$ is the ground acceleration, $\mathbf{M}$, $\mathbf{D}$, and $\mathbf{K}$ are the mass, damping, and stiffness matrices, $\mathbf{l}$ is the earthquake influence matrix, $\mathbf{T}_y$ is the matrix transforming the relative story displacements into inter-story drifts, and $\mathbf{I}$ is a unit matrix.

Properties of viscoelastic dampers

The VED is modeled by a linear spring and a dashpot arranged in parallel. Its stress–strain relation for a harmonic load is given by

$$\gamma = \gamma_0 \sin \omega t \tag{3}$$

$$\tau = G'(\omega)\gamma_0(\sin \omega t + \eta \cos \omega t) \tag{4}$$

where τ and γ are the shear stress and the shear strain of the damper, γ_0 and ω are the amplitude and the angular frequency of the harmonic shear strain, and $G'(\omega)$ and η are the storage modulus and the loss factor of the viscoelastic material [12]. From Equations (3) and (4), force–deformation relation can be induced as follows:

$$f = k_{\mathrm{d}} d + c_{\mathrm{d}} \dot{d} \tag{5}$$

$$d = t_{\mathrm{d}} \gamma \tag{6}$$

$$k_{\mathrm{d}} = v_{\mathrm{d}} G'(\omega) \tag{7}$$

$$c_{\mathrm{d}} = \frac{\eta}{\omega} k_{\mathrm{d}} \tag{8}$$

$$v_{\mathrm{d}} = \frac{A}{t_{\mathrm{d}}} \tag{9}$$

where d, f, A and t_{d} are the shear deformation, shear force, the area and the thickness of the damper, v_{d} is the ratio of the area to the thickness of the damper, and k_{d} and c_{d} are the stiffness and the damping coefficient for the harmonic load with angular frequency ω. The thickness t_{d} has a lower bound to prevent VED from shear failure. For a given value of v_{d}, the VED has minimum volume with the thickness of this lower bound and, therefore, v_{d} can play a role as a size parameter.

The properties of viscoelastic material used in this study are taken from the A-type VED used in the study of Chang *et al.* [13]. The storage stiffness of the A-type VED can be converted to the following storage modulus, $G'(\omega)$, with an additional scale factor, r:

$$G'(\omega) = \frac{r}{1898}\, e^{13.04} \left(\frac{\omega}{2\pi}\right)^{0.69} T^{-2.26} (\text{kN/cm}) \tag{10}$$

where T is the temperature of the damper (°C). It should be noted, however, that any other expression for the storage modulus can be employed in the proposed optimization scheme.

The stiffness and the damping coefficient of VED vary with the frequency of the deformation, ω, as can be seen from Equations (7), (8) and (10). Although dynamic loads such as earthquake and wind have a large number of frequency contents, in many structures, structural responses to those loads are dominated by a single vibration mode. Based on this observation, stiffness and damping coefficients of the VED are assumed to be constant and are calculated for the natural frequency of the dominant vibration mode.

State space representation of the damper–brace system

The damper–brace systems are installed between adjacent floors as shown in Figure 1. The VED and the brace are connected in series, while the former is composed of a linear spring and a dashpot connected in parallel, as shown in Figure 2, with the force–deformation relation of Equation (5). For such a damper–brace system, the overall force–deformation relation can be given by

$$\dot{f}_i = -\left(\frac{k_{\mathrm{d},i} + k_{\mathrm{b},i}}{c_{\mathrm{d},i}}\right) f_i + \left(\frac{k_{\mathrm{d},i} k_{\mathrm{b},i}}{c_{\mathrm{d},i}}\right) y_i + (k_{\mathrm{b},i})\dot{y}_i \tag{11}$$

$$y_i = (q_i - q_{i-1}) \cos\theta_i \tag{12}$$

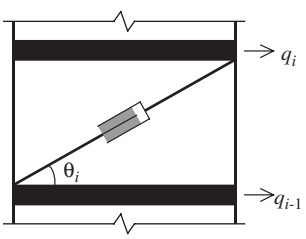

Figure 1. Configuration of a damper–bracesystem installed in a story.

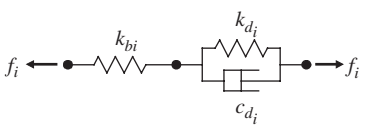

Figure 2. Mathematical modeling of a VED and a supporting brace.

where f_i and y_i are the control force and the deformation of the damper–brace system, respectively, q_i is the horizontal displacement of the i-th story, θ_i is the inclination angle of the brace, and $k_{\mathrm{b},i}, k_{\mathrm{d},i}$ and $c_{\mathrm{d},i}$ are the stiffness of the brace, the stiffness and damping coefficient of the VED, respectively. From the above equations, the state equation for the entire n damper–brace systems is given by

$$\dot{\mathbf{f}} = [\mathbf{A}_{\mathrm{f}}]\mathbf{f} + [\mathbf{B}_{\mathrm{f}1} \;\; \mathbf{B}_{\mathrm{f}2}] \begin{Bmatrix} \mathbf{y} \\ \dot{\mathbf{y}} \end{Bmatrix} \tag{13}$$

where $\mathbf{f}$ and $\mathbf{y}$ are the force vector and the deformation vector of n damper–brace systems and the component matrices are as follows:

$$\mathbf{A}_{\mathrm{f}} = -\mathrm{diag}\left\{ \frac{\omega_1}{\eta} \left(1 + \frac{k_{\mathrm{b},i}}{v_{\mathrm{d},i} G_i'(\omega_1)} \right) \right\} \tag{14}$$

$$\mathbf{B}_{\mathrm{f}1} = \mathrm{diag}\left\{ \frac{\omega_1}{\eta} k_{\mathrm{b},i} \right\} \tag{15}$$

$$\mathbf{B}_{\mathrm{f}2} = \mathrm{diag}\{k_{\mathrm{b},i}\} \tag{16}$$

where $\mathrm{diag}\{\cdot\}$ means the diagonal matrix, ω_1 is the frequency of the fundamental vibration mode and $v_{\mathrm{d},i}$ is the ratio of the area to the thickness for the i-th VED. The deformation vector of the damper–brace system, $\mathbf{y}$, is given by

$$\mathbf{y} = \mathbf{T}_{\mathrm{d}}\mathbf{q} \tag{17}$$

where $\mathbf{q}$ is the relative floor displacement vector and $\mathbf{T}_{\mathrm{d}}$ is expressed as follows

$$\mathbf{T}_{\mathrm{d}} = \begin{bmatrix} \cos\theta_1 & 0 & 0 & \cdots & 0 & 0 & 0 \\ -\cos\theta_2 & \cos\theta_2 & 0 & \cdots & 0 & 0 & 0 \\ \vdots & \vdots & \vdots & \ddots & \vdots & \vdots & \vdots \\ 0 & 0 & 0 & \cdots & 0 & -\cos\theta_n & \cos\theta_n \end{bmatrix} \tag{18}$$

State equations for input ground acceleration

The optimal distribution of dampers may be affected by the dynamic characteristics of excitation. In this study, the earthquake ground is modeled by the Kanai–Tagimi filter, of which the power spectral density (PSD) for the ground acceleration is given by

$$H_{\ddot{x}_g}(\omega) = \frac{1 + 4\xi_g^2(\omega/\omega_g)^2}{\{1 - (\omega/\omega_g)^2\}^2 + 4\xi_g^2(\omega/\omega_g)^2} S_{\mathrm{w}} \tag{19}$$

where ω_g and ξ_g are the natural frequency and the damping ratio of the soil, respectively, and S_{w} is the PSD of the white noise [14]. Since the Kanai–Tagimi filter is the single-degree-of-freedom (SDOF) oscillator subject to white noise input, it can be represented in the state

space form, so that it is combined with those of the model structure and the damper–brace system:

$$\dot{\mathbf{q}}_{\mathrm{w}} = \mathbf{A}_{\mathrm{w}}\mathbf{q}_{\mathrm{w}} + \mathbf{B}_{\mathrm{w}}w \tag{20}$$

$$\ddot{x}_g = \mathbf{C}_{\mathrm{w}}\mathbf{q}_{\mathrm{w}} + \mathbf{D}_{\mathrm{w}}w \tag{21}$$

where

$$\mathbf{A}_{\mathrm{w}} = \begin{bmatrix} 0 & 1 \\ -\omega_g^2 & -2\xi_g\omega_g \end{bmatrix} \tag{22}$$

$$\mathbf{B}_{\mathrm{w}} = \begin{bmatrix} 0 \\ -\sqrt{S_{\mathrm{w}}} \end{bmatrix} \tag{23}$$

$$\mathbf{C}_{\mathrm{w}} = [-\omega_g^2 \quad -2\xi_g\omega_g] \tag{24}$$

$$\mathbf{D}_{\mathrm{w}} = [0] \tag{25}$$

In this state space representation of the Kanai–Tagimi filter, $\mathbf{q}_{\mathrm{w}}$ is the state vector of the filter, w is the filter input which is white noise with unit PSD, $\ddot{x}_g$ is the ground acceleration, and ω_g and ξ_g are the natural frequency and the damping ratio of the filter, respectively.

State equations for a structure with added dampers

The augmented state and output equation including excitation model can be represented as follows:

$$\dot{\mathbf{x}} = \mathbf{A}_{\mathrm{c}}\mathbf{x} + \mathbf{B}_{\mathrm{c}}w \tag{26}$$

$$\mathbf{z} = \mathbf{C}_{\mathrm{c}}\mathbf{x} \tag{27}$$

where

$$\mathbf{x} = [\mathbf{q}^{\mathrm{T}} \;\; \dot{\mathbf{q}}^{\mathrm{T}} \;\; \mathbf{f}^{\mathrm{T}} \;\; \mathbf{q}_{\mathrm{w}}^{\mathrm{T}}]^{\mathrm{T}} \tag{28}$$

$$\mathbf{A}_{\mathrm{c}} = \begin{bmatrix} \mathbf{0} & \mathbf{I} & \mathbf{0} & \mathbf{0} \\ -\mathbf{M}^{-1}\mathbf{K} & -\mathbf{M}^{-1}\mathbf{D} & -\mathbf{M}^{-1}\mathbf{T}_{\mathrm{d}}^{\mathrm{T}} & -\mathbf{l}\mathbf{C}_{\mathrm{w}} \\ \mathbf{B}_{\mathrm{f1}}\mathbf{T}_{\mathrm{d}} & \mathbf{B}_{\mathrm{f2}}\mathbf{T}_{\mathrm{d}} & \mathbf{A}_{\mathrm{f}} & \mathbf{0} \\ \mathbf{0} & \mathbf{0} & \mathbf{0} & \mathbf{A}_{\mathrm{w}} \end{bmatrix} \tag{29}$$

$$\mathbf{B}_{\mathrm{c}} = [\mathbf{0} \;\; -\mathbf{D}_{\mathrm{w}}^{\mathrm{T}}\mathbf{l}^{\mathrm{T}} \;\; \mathbf{0} \;\; \mathbf{B}_{\mathrm{w}}^{\mathrm{T}}]^{\mathrm{T}} \tag{30}$$

$$\mathbf{C}_c = [\mathbf{T}_y \ \mathbf{0} \ \mathbf{0} \ \mathbf{0}] \tag{31}$$

$$\mathbf{T}_y = \begin{bmatrix} 1 & 0 & 0 & \cdots & 0 & 0 & 0 \\ -1 & 1 & 0 & \cdots & 0 & 0 & 0 \\ \vdots & \vdots & \vdots & \ddots & \vdots & \vdots & \vdots \\ 0 & 0 & 0 & \cdots & 0 & -1 & 1 \end{bmatrix} \tag{32}$$

The state vector of the augmented state equation is composed of floor displacements $\mathbf{q}$, floor velocities $\dot{\mathbf{q}}$, control forces in damper–brace systems $\mathbf{f}$, and the two filter states $\mathbf{q}_w$. The input of the equation is the white noise, and the output of the equation is composed of the n inter-story drifts of the structure. In case the number of stories and the number of state variables of the structure become very large, the size of the state equation can be reduced by including only a few dominant vibration modes in Equation (1).

ESTIMATION OF THE MAXIMUM RESPONSES

The primary purpose of adding VEDs in a structure subjected to an earthquake load is to reduce the structural response below a critical limit state. Therefore, in the proposed optimization procedure, constraints are imposed on the maximum responses of the structure. For this purpose, a simple procedure for predicting the maximum responses for the design earthquake is necessary. Owing to the statistical nature of earthquake loads, the maximum responses are also defined statistically.

In this study, the earthquake excitation is modeled by the Kanai–Tagimi power spectral density function, shown in Equation (19). The mean value of the maximum response for this type of excitation is obtained by multiplying the root mean square (RMS) response by a peak factor. Based on the probability distribution function of the peak values for the stationary Gaussian random process proposed by Vanmarke [15], Kiureghian [16] proposed the following equations for the mean of maximum response by modifying the peak factor given by Davenport [17]:

$$\mu_y = p\sigma_y \tag{33}$$

$$p = \sqrt{2 \ln v_e \tau} + \frac{0.5772}{\sqrt{2 \ln v_e \tau}} \tag{34}$$

where μ_y is the mean of the maximum response, p is the peak factor, σ_y is the variance of the response, v_e is the modified mean zero-crossing rate, and τ is the duration time of the excitation. Kiureghian derived the simple expression of v_e for a SDOF system subjected to white noise ground acceleration:

$$v_e = \begin{cases} (1.90\xi^{0.15} - 0.73)v; & (\xi < 0.54) \\ v; & (\xi \geqslant 0.54) \end{cases} \tag{35}$$

where

$$v = \frac{\omega_0}{\pi} \tag{36}$$

in which v is the zero-crossing rate of the response, and ω_0 and ξ are the natural frequency and the damping ratio of the SDOF structure, respectively. He also showed that the above coefficient can be applied to the white noise excitation which is passed through the Kanai–Tagimi filter as long as the natural frequency of the SDOF structure is within the frequency band of the filter [18].

For the multi-degree-of-freedom (MDOF) structure, the natural frequency and the damping ratio of the fundamental vibration mode are used in Equations (35) and (36) under the assumption that the fundamental mode dominates the dynamic response, which is rational for many of the regular building structures.

OPTIMAL DESIGN OF VED AND SUPPORTING BRACES

Design objective and constraints

In this study the primary objective of installing VEDs is determined to reduce inter-story drifts below given target values. There can exist, however, a lot of combinations of the size of VED and the stiffness of supporting braces that satisfy the given design objective. Therefore, through the optimization procedure it is intended to find the case that minimizes both design parameters while satisfying the constraints on the inter-story drifts. To this end, a quadratic function of the VED size and supporting brace stiffness is chosen as an objective function. Also, inequality constraints on every inter-story drift of interest are provided, and finally the optimization problem can be represented as follows:

$$\text{minimize } f(\mathbf{v}_\mathrm{d}, \mathbf{k}_\mathrm{b}) = \sum_{i=1}^{n} v_{\mathrm{d},i}^2 + \alpha \sum_{i=1}^{n} k_{\mathrm{b},i}^2 \tag{37}$$

subjected to

$$\dot{\mathbf{x}} = \mathbf{A}_\mathrm{c}\mathbf{x} + \mathbf{B}_\mathrm{c} w \tag{38}$$

$$z_i = \mathbf{C}_{\mathrm{c},i}\mathbf{x} \leqslant z_{\max,i} \ (i = 1, \ldots, n) \tag{39}$$

where α is a weighting factor, $\mathbf{C}_{\mathrm{c},i}$ is the i-th row of $\mathbf{C}_\mathrm{c}$, $z_{\max,i}$ is the critical value of the i-th inter-story drift, and $\mathbf{v}_\mathrm{d}$ and $\mathbf{k}_\mathrm{b}$ are vectors of the VED size parameters, $v_{\mathrm{d},i}$, and the supporting brace stiffness, $k_{\mathrm{b},i}$, respectively. The α in Equation (37) works not only as a weighting factor but also as a scaling factor between two physically different quantities, $v_{\mathrm{d},i}$ and $k_{\mathrm{b},i}$.

The equality constraint, Equation (38), is associated with the dynamics of the overall structure including the VED and the excitation filter. Since the dynamic response of the structure is evaluated stochastically, this constraint equation can be substituted by the following Lyapunov equation under the assumption that the input excitation, w, of Equation (38) is of white noise with the power spectral density of 1.0:

$$\mathbf{A}_\mathrm{c}\mathbf{P} + \mathbf{P}\mathbf{A}_\mathrm{c}^\mathrm{T} + \mathbf{B}_\mathrm{c}\mathbf{B}_\mathrm{c}^\mathrm{T} = \mathbf{0} \tag{40}$$

where $\mathbf{P}$ is the covariance matrix of the state variable $\mathbf{x}$, and plays a role as an additional independent design variable.

The n inequality constraints, Equation (39), which are associated with the maximum inter-story drifts, can be expressed by the following single equation using the RMS values of the

inter-story drifts and the peak factor p of Equation (34) as follows:

$$g(\mathbf{P}) = \max_i \left(\frac{p\sqrt{E[z_i^2]}}{z_{\max,i}} \right)^2 - 1$$

$$= \max_i \left(\frac{p\sqrt{\mathbf{C}_{c,i}\mathbf{P}\mathbf{C}_{c,i}^{\mathrm{T}}}}{z_{\max,i}} \right)^2 - 1 \leqslant 0 \tag{41}$$

This provides the advantage that the number of Lagrange multipliers associated with the constraint equations is reduced from n, the number of stories, to 1. Also, the satisfaction of the inequality constraint, Equation (41), implies that the equality constraints are also satisfied, because the calculation of $g(\mathbf{P})$ requires the solution of the Lyapunov equation (Equation (40)) which is none other than the equality constraint. As a result, the equality constraint, the related additional design variable, $\mathbf{P}$, and Lagrange multipliers can be removed from the optimization problem. Since the number of Lagrange multipliers related to the equality constraint has the order of the square of the total number of states in the augmented state equation, Equation (26), the optimization procedure is simplified significantly as a result of employing Equation (41). Consequently, the optimization problem can be reduced as follows with only two independent design variables $\mathbf{v}_d$ and $\mathbf{k}_b$:

$$\min f(\mathbf{v}_d, \mathbf{k}_b) \tag{42}$$

$$\text{sub. to } g(\mathbf{v}_d, \mathbf{k}_b) \leqslant 0 \tag{43}$$

where $g(\mathbf{v}_d, \mathbf{k}_b)$ is another form of $g(\mathbf{P})$, which can be understood considering the fact that $\mathbf{P}$ becomes the function of $\mathbf{v}_d$ and $\mathbf{k}_b$, as can be seen in Equation (40). The Lagrangian and the Kuhn–Tucker optimality condition of the optimization problem can be represented as follows:

$$L(\mathbf{v}_d, \mathbf{k}_b) = f(\mathbf{v}_d, \mathbf{k}_b) - \lambda \cdot g(\mathbf{v}_d, \mathbf{k}_b) \tag{44}$$

$$\frac{\partial L}{\partial \mathbf{v}_d} = \frac{\partial f}{\partial \mathbf{v}_d} - \lambda \frac{\partial g}{\partial \mathbf{v}_d} = 0 \tag{45}$$

$$\frac{\partial L}{\partial \mathbf{k}_b} = \frac{\partial f}{\partial \mathbf{k}_b} - \lambda \frac{\partial g}{\partial \mathbf{k}_b} = 0 \tag{46}$$

$$\lambda \cdot g(\mathbf{v}_d, \mathbf{k}_b) = 0 \tag{47}$$

$$\lambda \geqslant 0 \tag{48}$$

where λ is the Lagrange multiplier for the inequality constraint. Because one of the purposes of the present study is to investigate the effect of supporting braces on the performance of the VED, constraints on the upper bound of the supporting brace stiffness is also imposed on the optimization procedure.

Gradients of design variables and constraint equations

Algorithms to solve the non-linear optimization problem defined by Equations (42) and (43) are grouped into gradient-based methods and direct search methods. For the problem with a

large number of design variables, the former is known to be more effective than the latter if the gradients of the objective function and constraints are continuous [19]. Therefore, in this section, the gradients necessary to solve the optimization problem are derived so that they can be applied easily in program codes for optimum design.

The gradients of the objective function with respect to the design variables such as VED size parameters and brace stiffness are as follows:

$$\frac{\partial f}{\partial v_{\mathrm{d},i}} = 2 \sum_{i=1}^{n} v_{\mathrm{d},i} \tag{49}$$

$$\frac{\partial f}{\partial k_{\mathrm{b},i}} = 2\alpha \cdot \sum_{i=1}^{n} k_{\mathrm{b},i} \tag{50}$$

The gradients of the non-linear constraint equations can be expressed as follows using the chain rule:

$$\frac{\partial g}{\partial v_{\mathrm{d},i}} = \sum_{p=1}^{n} \sum_{q=1}^{n} \frac{\partial g}{\partial \mathbf{P}_{pq}} \frac{\partial \mathbf{P}_{pq}}{\partial v_{\mathrm{d},i}} \tag{51}$$

$$\frac{\partial g}{\partial k_{\mathrm{b},i}} = \sum_{p=1}^{n} \sum_{q=1}^{n} \frac{\partial g}{\partial \mathbf{P}_{pq}} \frac{\partial \mathbf{P}_{pq}}{\partial k_{\mathrm{b},i}} \tag{52}$$

where $\mathbf{P}_{pq}$ represents the (p,q)-th element of the matrix $\mathbf{P}$. In Equations (51) and (52), the gradient of the constraint equation, g, with respect to the element of the covariance matrix $\mathbf{P}$ of the state variable can be obtained from the following gradient matrix:

$$\left[\frac{\partial g}{\partial \mathbf{P}}\right] = \frac{\partial}{\partial \mathbf{P}} \left(\frac{p^2}{z_{\max,i}^2} \cdot \mathrm{trace}(\mathbf{C}_{\mathrm{c},i} \mathbf{P} \mathbf{C}_{\mathrm{c},i}^{\mathrm{T}}) \right) = \frac{p^2}{z_{\max,i}^2} \mathbf{C}_{\mathrm{c}_i}^{\mathrm{T}} \mathbf{C}_{\mathrm{c}_i} \tag{53}$$

where a differentiation rule for the trace of the matrix is used. The peak factor, p, in this equation is the function of the natural frequency and the damping ratio of the structure, which are changed by the installation of the VED. Therefore it should be differentiated in the computation of the gradient matrix. However, as it is too complex to derive the closed-form solution of the gradient, the peak factor p is assumed to be constant during each iteration step assuming that its variation is small.

The gradient matrices of the covariance matrix $\mathbf{P}$ with respect to the design variables shown in Equations (51) and (52) can be computed from other Lyapunov equations which are obtained by the differentiation of the implicit constraint equation, Equation (40), with respect to the design variables:

$$\mathbf{A}_{\mathrm{c}} \left[\frac{\partial \mathbf{P}}{\partial v_{\mathrm{d}_i}}\right] + \left[\frac{\partial \mathbf{P}}{\partial v_{\mathrm{d}_i}}\right] \mathbf{A}_{\mathrm{c}}^{\mathrm{T}} + \left\{ \left[\frac{\partial \mathbf{A}_{\mathrm{c}}}{\partial v_{\mathrm{d}_i}}\right] \mathbf{P} + \mathbf{P} \left[\frac{\partial \mathbf{A}_{\mathrm{c}}}{\partial v_{\mathrm{d}_i}}\right]^{\mathrm{T}} \right\} = \mathbf{0} \tag{54}$$

$$\mathbf{A}_{\mathrm{c}} \left[\frac{\partial \mathbf{P}}{\partial k_{\mathrm{b}_i}}\right] + \left[\frac{\partial \mathbf{P}}{\partial k_{\mathrm{b}_i}}\right] \mathbf{A}_{\mathrm{c}}^{\mathrm{T}} + \left\{ \left[\frac{\partial \mathbf{A}_{\mathrm{c}}}{\partial k_{\mathrm{b}_i}}\right] \mathbf{P} + \mathbf{P} \left[\frac{\partial \mathbf{A}_{\mathrm{c}}}{\partial k_{\mathrm{b}_i}}\right]^{\mathrm{T}} \right\} = \mathbf{0} \tag{55}$$

In these Lyapunov equations, the derivatives of the matrix $\mathbf{A}_c$ with respect to the design variables are obtained by the differentiation of its component matrix as follows:

$$\left[\frac{\partial \mathbf{A}_c}{\partial v_{d,i}}\right] = \begin{bmatrix} \mathbf{0} & \mathbf{0} & \mathbf{0} & \mathbf{0} \\ \mathbf{0} & \mathbf{0} & \mathbf{0} & \mathbf{0} \\ \mathbf{0} & \mathbf{0} & \left[\dfrac{\partial \mathbf{A}_f}{\partial v_{d,i}}\right] & \mathbf{0} \\ \mathbf{0} & \mathbf{0} & \mathbf{0} & \mathbf{0} \end{bmatrix} \tag{56}$$

$$\left[\frac{\partial \mathbf{A}_c}{\partial k_{b,i}}\right] = \begin{bmatrix} \mathbf{0} & \mathbf{0} & \mathbf{0} & \mathbf{0} \\ \mathbf{0} & \mathbf{0} & \mathbf{0} & \mathbf{0} \\ \left[\dfrac{\partial \mathbf{B}_{f1}}{\partial k_{b,i}}\right]\mathbf{T}_d & \left[\dfrac{\partial \mathbf{B}_{f2}}{\partial k_{b,i}}\right]\mathbf{T}_d & \left[\dfrac{\partial \mathbf{A}_f}{\partial k_{b,i}}\right] & \mathbf{0} \\ \mathbf{0} & \mathbf{0} & \mathbf{0} & \mathbf{0} \end{bmatrix} \tag{57}$$

where

$$\left[\frac{\partial \mathbf{A}_f}{\partial v_{d,i}}\right]_{pq} = \begin{cases} \dfrac{\omega_1 k_{b,i}}{\eta v_{d,i}^2 G_i'(\omega_1)} & (\text{if } \ p=q=i) \\ 0 & (\text{otherwise}) \end{cases} \tag{58}$$

$$\left[\frac{\partial \mathbf{A}_f}{\partial k_{b,i}}\right]_{pq} = \begin{cases} -\dfrac{\omega_1}{\eta v_{d,i} G_i'(\omega_1)} & (\text{if } \ p=q=i) \\ 0 & (\text{otherwise}) \end{cases} \tag{59}$$

$$\left[\frac{\partial \mathbf{B}_{f1}}{\partial k_{b,i}}\right]_{pq} = \begin{cases} \dfrac{\omega_1}{\eta} & (\text{if } \ p=q=i) \\ 0 & (\text{otherwise}) \end{cases} \tag{60}$$

$$\left[\frac{\partial \mathbf{B}_{f2}}{\partial k_{b,i}}\right]_{pq} = \begin{cases} 1 & (\text{if } \ p=q=i) \\ 0 & (\text{otherwise}) \end{cases} \tag{61}$$

NUMERICAL EXAMPLE

Analysis model

The model structure for numerical analysis, shown in Figure 3, is an 8-story shear building with the story mass and the story stiffness of 3.456×10^6 kg and 3.404×10^6 kN/m, respectively. The natural frequency of the first mode is 0.92 Hz, and all the damping ratios are assumed to be 2% of the critical damping. VEDs are installed between two adjacent floors, and the configuration of VEDs and supporting braces installed are depicted in Figure 1.

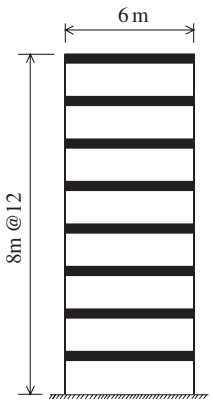

Figure 3. Model structure for numerical example.

Characteristics of viscoelastic dampers

The properties of viscoelastic material are based on the study of Chang *et al.* as mentioned previously. The storage modulus, $G'(\omega)$, of the viscoelastc material is obtained from Equation (10) and the scale factor, r, is assumed to be 100.0. The loss factor, η, is assumed to be 1.12. The natural frequency of the fundamental structural vibration mode is used for ω in the computation of the stiffness and the damping coefficients of each VED. However, as the natural frequency of the structure is changed as a result of the installation of VEDs, the coefficients are calculated by iteration. For this example, five iterations are required to obtain a converged value. The thickness of all VEDs is assumed to be 2.6 cm and the area of the each VED is determined from the corresponding optimized size parameter, $v_{\mathrm{d},i}$.

Ground acceleration

For the modeling of ground acceleration employing the Kanai–Tagimi filter, the natural frequency, ω_g, and the damping ratio, ξ_g, of the soil are assumed to be 15.6 rad/sec and 0.6, respectively, as Kanai suggested for the firm soil condition [14]. The power spectral density of the white noise filter input, S_{w}, is determined so that the mean value of the peak ground accelerations becomes 1.0 g. A total of 100 ground acceleration time histories were generated for analysis by filtering the white noise input with variance of 1.0 through the Kanai–Tagimi filter.

Design cases

The optimization has been carried out in four different design cases. The design case I assumes that all the supporting braces have infinite stiffness. For this purpose, the stiffness of each brace is set to be 1000 times the story stiffness. On the other hand, design case II assumes finite stiffness for all supporting braces. In design case III, the stiffness of supporting braces is included in the design variables with inequality constraints on their upper bounds. In these three design cases, only size parameters, $v_{\mathrm{d}i}$, are included in the objective function (Equation (37)). That is, the weighting, α, is set to be zero. Design case IV has the same design conditions as the previous case except that the stiffness of supporting braces is included in the objective function. In this case the weighting factor α is determined by trial and error to get similar sizes of VED to the previous three design cases. Table I summarizes the objective

Table I. Design cases for optimization.

Design case	Objective functions	Design variables	Constraint on brace stiffness
I	Sum of squared VED size parameters	Size parameters of VED	Infinite
II	Sum of squared VED size parameters	Size parameters of VED	Fixed value
III	Sum of squared VED size parameters	Size parameters of VED and brace stiffness	Upper-bound
IV	Sum of squared VED size parameters and brace stiffness	size parameters of VED and brace stiffness	Upper-bound

functions, design variables, and constraints associated with the four design cases. For each design case, two levels of constraints on inter-story drifts, 60% and 30% of the maximum inter-story drift of the structure before VEDs are installed, are imposed to investigate the relation between size of VED and stiffness of supporting brace. The former response constraint is denoted as constraint *A* and the latter as constraint *B*.

Result of optimization for response constraint A

In this study the sequential quadratic programming algorithm provided in the Optimization Toolbox of MATLAB is used for the optimization. The optimized size of VED for response constraint *A* is plotted in Figures 4(a) and (b), where the area of VED for the fixed thickness of 2.6 cm is presented. The upper bounds for the stiffness of supporting braces are set to be 2 and 64 times the story stiffness. These values for upper bounds are also applied for the design case II as the fixed stiffness of supporting braces. It can be observed that most of the VEDs are concentrated in the lower stories where inter-story drifts are large. When the upper bound of brace stiffness is set to be 64 times the story stiffness, there is only a small difference whether the brace stiffness is limited or not, as shown in Figure 4(a). However, when the upper bound of the brace stiffness is set to be twice the story stiffness, the amounts of VED installed in the design cases II, III and IV, for which the brace stiffness is limited, are considerably larger than the design case I with infinite brace stiffness, as shown in Figure 4(b).

The results of optimization for supporting braces are presented in Figure 5. When the upper bound of the brace stiffness is set to be 64 times the story stiffness, the result of design case IV, in which the brace stiffness as well as the VED size is included in the objective function, achieves response reduction ratio with a considerably small brace stiffness, as depicted in Figure 5 (a). However, the increase of the VED size in compensation for the decrease of brace stiffness is insignificant as can be seen in Figure 4(a). This implies that although the use of stiffer supporting braces may be beneficial to increase the effectiveness of VED and to reduce the structural response, it is not cost effective to use brace stiffness larger than the optimum value.

On the other hand, when the upper bound of the brace stiffness is set to be twice the story stiffness, brace stiffness corresponding to the installed VED reached the upper bound. Therefore, when sufficient brace stiffness cannot be supplied, it needs to be fixed to the upper bound and the optimization procedure should be carried out considering only VED.

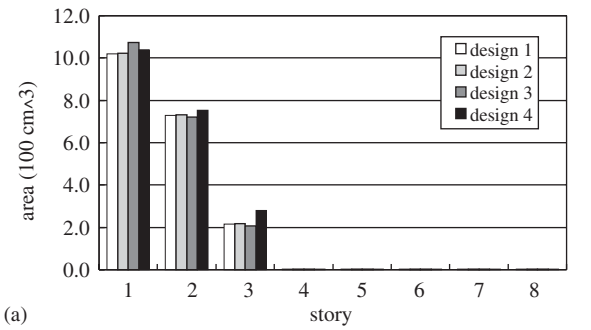

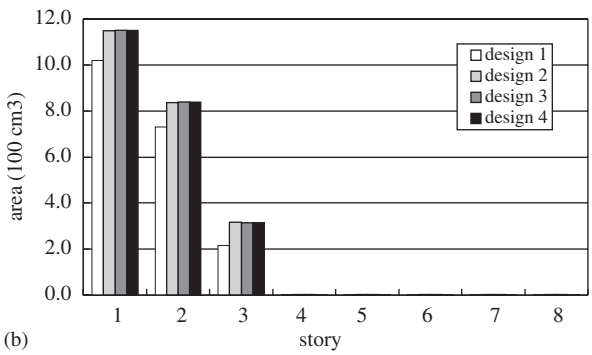

Figure 4. Result of optimization for VED for response constraint *A*: (a) high upper bound for brace stiffness (64 times the story stiffness); and (b) low upper bound for brace stiffness (twice the story stiffness).

Result of optimization for response constraint B

The results of four design cases with constraint *B* are presented in Figures 6 to 8. The results of optimum VED size are plotted in Figure 6, where the upper bounds for brace stiffness are the same as those for the case of response constraint *A*. In design case I, in which brace stiffness is assumed to be infinite, no damper is allocated to upper stories. On the other hand, in the other three design cases, in which brace stiffness is limited to finite values, VED is installed in all stories for the low upper bound of brace stiffness, as shown in Figure 6(b). Also, it can be observed in Figures 6(a) and (b) that the size of VED increases significantly if the brace stiffness is limited to twice the story stiffness. Therefore, the number of stories in which VED is assigned and the size of VED depends highly on the brace stiffness, if strong constraints on responses are imposed.

Figure 7 represents the results of optimization for brace stiffness. When the upper bound of brace stiffness is set to be 64 times the story stiffness, then design case IV, in which the brace stiffness as well as VED size is included in the objective function, satisfies the constraint on the response with brace stiffness well below the upper limit. As in the case for constraint *A*, the increase in the size of VED in compensation for the decrease in brace stiffness is insignificant as can be observed in Figure 6(a). On the other hand, when the upper bound for brace stiffness is set to be twice the story stiffness, the stiffness of braces determined from

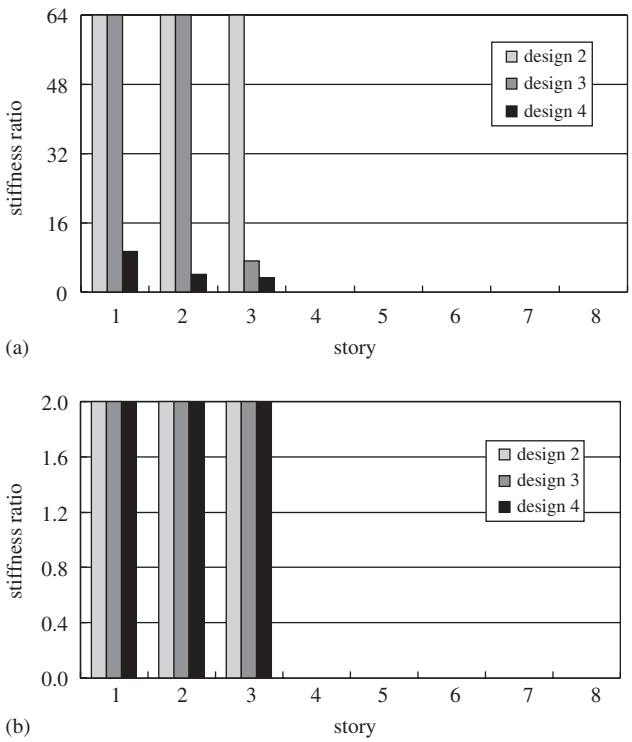

Figure 5. Result of optimization for supporting braces (response constraint *A*): (a) high upper bound for brace stiffness (64 times the story stiffness); and (b) low upper bound for brace stiffness (twice the story stiffness).

the optimization process reaches the upper bound in all design cases, as in the design cases for constraint *A*.

Figure 8 shows the reduction in the maximum inter-story drifts when VEDs and supporting braces are designed for response constraint *B* with the upper bound of brace stiffness twice the story stiffness. Maximum inter-story drifts are calculated using the peak factor of Equation (34) and are normalized to the first inter-story drift of the original structure. To simulate the conventional practice of designing VED, optimization was processed assuming that the brace stiffness in design case I is infinite. Then in the computation of the inter-story drift, the realistic value for the brace stiffness, which is twice the story stiffness, was used. The results show that, owing to the insufficiency of brace stiffness, the maximum inter-story drift obtained for design case I turned out to be 38.6% of the maximum inter-story drift of the original structure, which exceeds the prescribed value of 30 % for response constraint *B*. This implies that if the flexibility of the supporting brace is not considered in the design of the VED, the actual maximum responses may be larger than those predicted from analysis.

Accuracy of the peak response

Table II shows the maximum inter-story drifts of the model structure averaged from the results of 100 simulations. VED and brace stiffness are optimized for design case IV with various

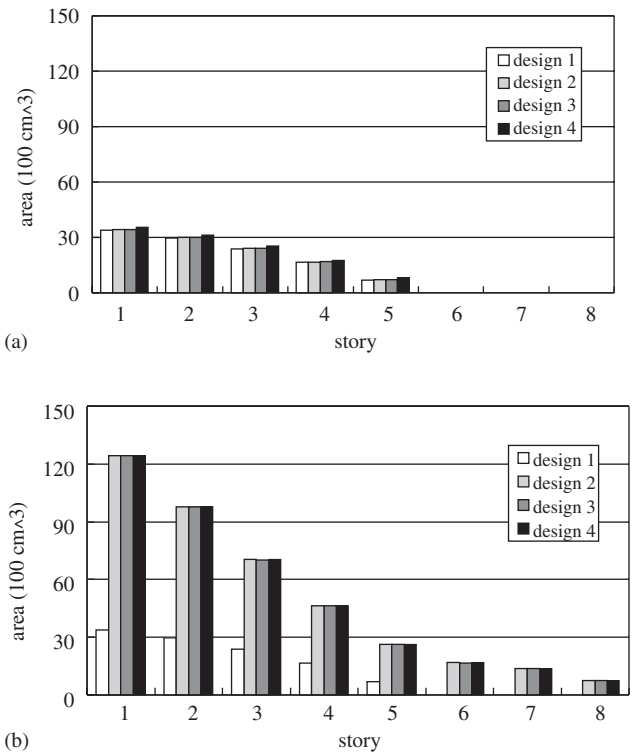

Figure 6. Result of optimization for VED (response constraint *B*): (a) high upper bound for brace stiffness (64 times the story stiffness); and (b) low upper bound for brace stiffness (twice the story stiffness).

upper bounds on brace stiffness. Ground acceleration time histories were generated by passing white noise input through the Kanai–Tagimi filter. The time histories have mean peak ground acceleration of 1.0 g and duration of 20 seconds, and a sample record is plotted in Figure 9. The values in the parentheses in Table II denote the ratio of the maximum response averaged from the simulation results to the mean maximum response calculated using the peak factor defined in Equation (34). It can be observed that the mean responses of the original structure (without VED) are 92% of the estimated value, whereas the accuracy reaches close to 100% when VEDs are installed. The reason for the relatively large difference in the original structure seems to be due to the fact that the peak factor used in the estimation of the response is based on the fundamental vibration mode, and thus the higher mode effects inherent in the MDOF structure are not taken into account. On the other hand, when VEDs are installed, the accuracy of the responses estimated using Equation (34) increases since VED suppresses higher mode effect in the total structural responses.

Figures 10 and 11 represent sample time histories of inter-story drift of the model structure for the response constraints *A* and *B*, respectively. In both figures the upper limit for the brace stiffness is set to be 64 times story stiffness. It can be observed in these figures that the maximum responses satisfy the given constraints quite well.

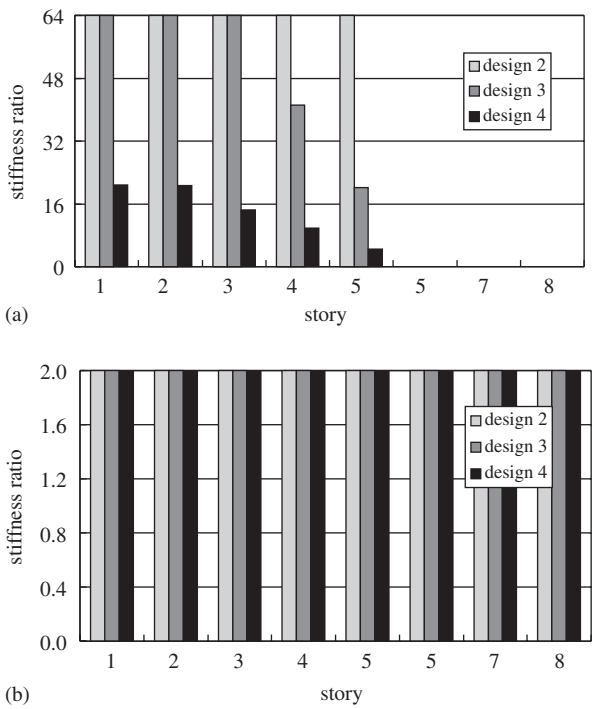

Figure 7. Result of optimization for supporting braces (response constraint B): (a) high upper bound for brace stiffness (64 times the story stiffness); and (b) low upper bound for brace stiffness (twice the story stiffness).

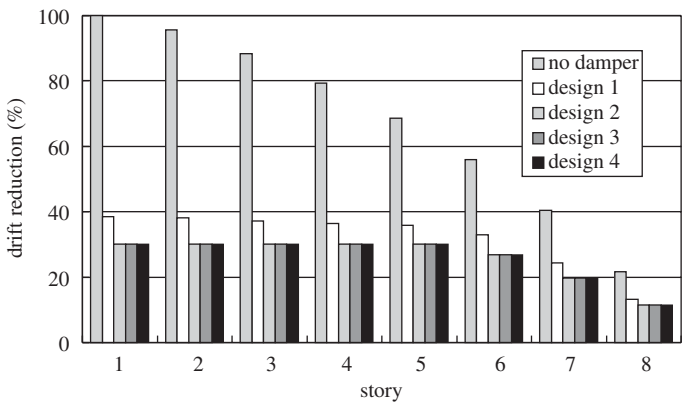

Figure 8. Normalized maximum inter-story drifts of the model structure (response constraint B).

Variation of the peak factor in the optimization process

One of the problems encountered in the proposed optimization procedure is that it is hard to derive the closed-form solution for the gradient of the objective functions and constraints taking the variation of the peak factor into account. In this study, the peak factor was assumed

Table II. Mean maximum inter-story drift for design case IV (unit: cm).

	Brace stiffness/ story stiffness	Without VED	Response constraint *A*	Response constraint *B*
Estimation	—	0.1238 (1.00)	0.0743 (1.00)	0.0371 (1.00)
Simulation result	2	0.1137 (0.92)	0.0740 (0.99)	0.0369 (0.99)
	4		0.0732 (1.02)	0.0377 (1.02)
	8		0.0721 (1.01)	0.0374 (1.01)
	16		0.0733 (1.01)	0.0374 (1.01)
	32		0.0731 (0.97)	0.0359 (0.97)
	64		0.0728 (1.01)	0.0375 (1.01)

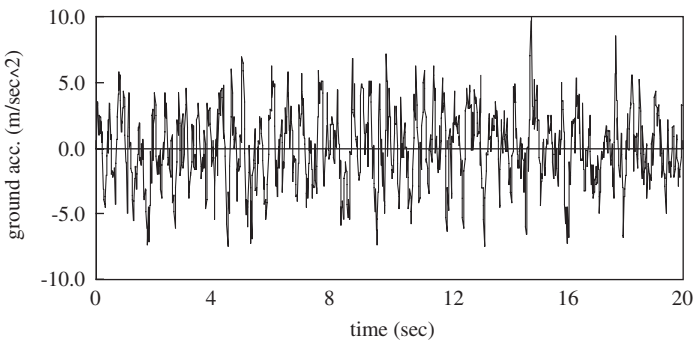

Figure 9. Sample ground acceleration history.

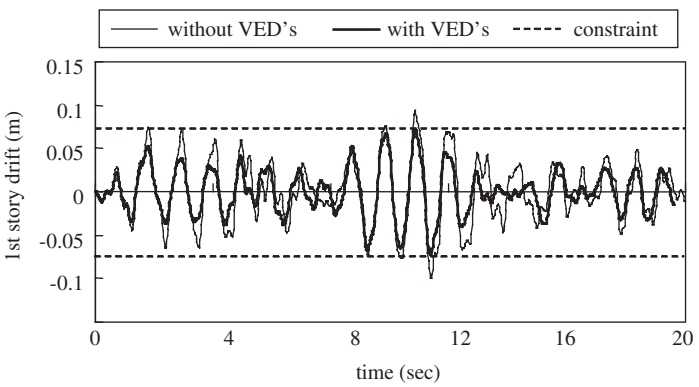

Figure 10. First inter-story drift of the model structure (response constraint *A*).

to be constant in the calculation of the gradients on the assumption that the peak factor varies slowly in each computation step. To verify this assumption, the variation of the peak factor in each iteration step is plotted in Figure 12, where design case IV and response constraint *A* are applied and the upper bound of brace stiffness is set to be 64 times the story stiffness. The result shows that the peak factor converges to a constant value. Although there are several

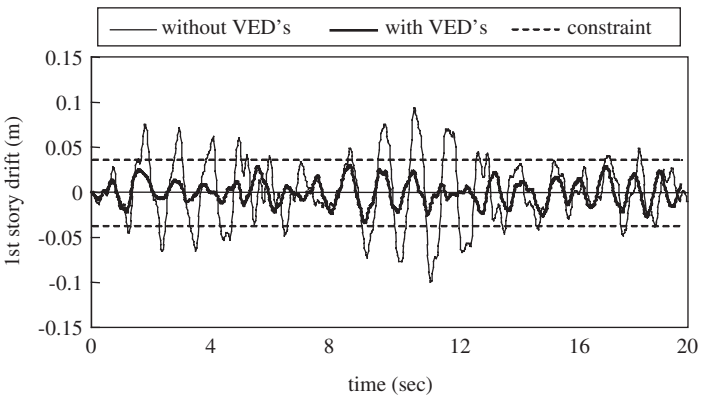

Figure 11. First inter-story drift of the model structure (response constraint B).

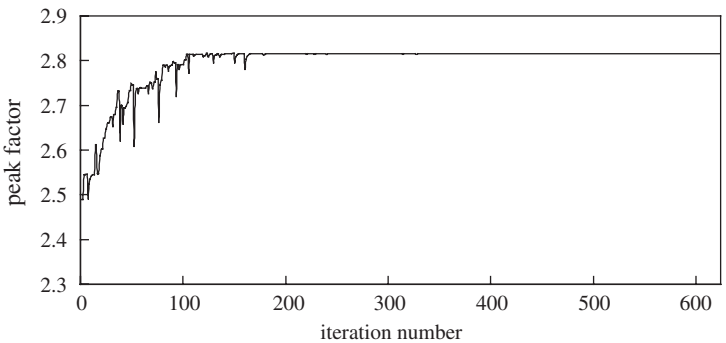

Figure 12. Variation of the peak factor.

points where the peak factor changes abruptly, the overall trend of change is quite smooth and the amount of change is only 13% of the initial value. Therefore the assumption made on the variation of the peak factor seems to be reasonable.

CONCLUSION

This study presents a simultaneous optimization procedure for VED and the supporting braces, and the effect of the flexibility of a supporting brace on the required VED size was investigated. For the optimization, the system of VED with a supporting brace was modeled by a state equation, which was combined with that of the structure. Also, the maximum response of the structure, which is more practical than the RMS response for design purposes, was represented using the stochastic peak factor.

The analysis results showed that when sufficient stiffness cannot be provided for the supporting braces, which happens frequently in practice for functional or architectural reasons, the flexibility of the brace should be taken into account in the optimization process to meet the given constraints for structural responses. By the simultaneous optimization procedure, the

size of the supporting brace could be reduced without significant increase in the size of VED. Also the same level of safety could be achieved with a smaller amount of supporting brace by applying the optimization procedure.

ACKNOWLEDGEMENTS

This work was supported by the fund of the National Research Laboratory Program (Project No. M1-0203-00-0068) from the Ministry of Science and Technology in Korea. The authors appreciate this financial support.

REFERENCES

1. Zhang R, Soong TT. Seismic design of viscoelastic dampers for structural applications. *Journal of Structural Engineering* (ASCE) 1992; **118**:1375–1392.
2. Shukla AK, Datta TK. Optimal use of viscoelastic dampers in building frames for seismic force. *Journal of Structural Engineering* (ASCE) 1999; **125**:401–409.
3. Gluck N, Reinhorn AM, Gluck J, Levy R. Design of supplemental dampers for control of structures. *Journal of Structural Engineering* (ASCE) 1996; **122**:1394–1399.
4. Loh C-H, Lin P-Y, Chung N-H. Design of dampers for structures based on optimal control theory. *Earthquake Engineering and Structural Dynamics* 2000; **29**:1307–1323.
5. Tsuji M, Nakamura T. Optimum viscous dampers for stiffness design of shear buildings. *Structural Design of Tall Buildings* 1996; **5**:217–234.
6. Takewaki I. Optimal damper placement for minimum transfer functions. *Earthquake Engineering and Structural Dynamics* 1997; **26**:1113–1124.
7. Singh MP, Moreschi LM. Optimal seismic response control with dampers. *Earthquake Engineering and Structural Dynamics* 2001; **30**:553–572.
8. Moreschi LM, Singh MP. Optimal placement of dampers for passive response control. *Earthquake Engineering and Structural Dynamics* 2002; **31**:955–976.
9. Hwang J-S, Min K-W, Hong S-M. Optimal design of passive viscoelastic dampers having active control effect for building structures. *Transactions of the Korean Society for Noise and Vibration Engineering* (KSNVE) 1995; **5**(2):225–234.
10. Fu Y, Kasai K. Comparative study of frames using viscoelastic and viscous dampers. *Journal of Structural Engineering* (ASCE) 1998; **124**(5):513–522.
11. Takewaki I, Yoshitomi S. Effects of support stiffness on optimal damper placement for a planar building frame. *Structural Design of Tall Buildings* 1998; **7**:323–336.
12. Zhang R-H, Soong TT, Mahmoodi P. Seismic response of steel frame structures with added viscoelastic dampers. *Earthquake Engineering and Structural Dynamics* 1989; **18**:389–396.
13. Chang KC, Soong TT, Oh S-T, Lai ML. Seismic behavior of steel frame with added viscoelastic dampers. *Journal of Structural Engineering* (ASCE) 1995; **121**:1418–1426.
14. Clough RW, Penzien J. *Dynamics of Structures*; McGraw-Hill: New York, NY, 1993.
15. Vanmarke EH. Properties of spectral moments with applications to random vibration. *Journal of the Engineering Mechanics Division* (ASCE) 1972; **98**(EM2):425–446.
16. Kiureghian AD. Structural response to stationary excitation. *Journal of the Engineering Mechanics Division* (ASCE) 1980; **106**(EM6):1195–1213.
17. Davenport AG. Note on the distribution of the largest value of a random function with application to gust loading. *Proceedings of the Institution of Civil Engineers*, London, Vol. **28**:187–196, 1964.
18. Kiureghian AD. A response spectrum method for random vibration analysis of MDF systems. *Earthquake Engineering and Structural Dynamics* 1981; **9**:419–435.
19. Belegundu AD, Chandruptla TR. *Optimization Concepts and Applications in Engineering*; Prentice Hall, 1999.

